



**HAL**  
open science

# High-fidelity models for the online control of power ramps in fuel displacement systems – Revisiting the ISABELLE experiment in the OSIRIS Material Testing Reactor

Yifan Peng, David Blanchet, Robert Jacqmin, Jérôme Julien, Joël Rosato

► **To cite this version:**

Yifan Peng, David Blanchet, Robert Jacqmin, Jérôme Julien, Joël Rosato. High-fidelity models for the online control of power ramps in fuel displacement systems – Revisiting the ISABELLE experiment in the OSIRIS Material Testing Reactor. EPJ N - Nuclear Sciences & Technologies, 2024, 10, pp.3. 10.1051/epjn/2024001 . hal-04549055

**HAL Id: hal-04549055**

**<https://hal.science/hal-04549055>**

Submitted on 16 Apr 2024

**HAL** is a multi-disciplinary open access archive for the deposit and dissemination of scientific research documents, whether they are published or not. The documents may come from teaching and research institutions in France or abroad, or from public or private research centers.

L'archive ouverte pluridisciplinaire **HAL**, est destinée au dépôt et à la diffusion de documents scientifiques de niveau recherche, publiés ou non, émanant des établissements d'enseignement et de recherche français ou étrangers, des laboratoires publics ou privés.



Distributed under a Creative Commons Attribution 4.0 International License

# High-fidelity models for the online control of power ramps in fuel displacement systems – Revisiting the ISABELLE experiment in the OSIRIS Material Testing Reactor

Yifan Peng<sup>1</sup>, David Blanchet<sup>1,\*</sup>, Robert Jacqmin<sup>1</sup>, Jérôme Julien<sup>1</sup>, and Joël Rosato<sup>2</sup>

<sup>1</sup> CEA Cadarache, DES/IRESNE/DER, 13108 Saint-Paul-lez-Durance, France

<sup>2</sup> Aix Marseille University, CNRS, PIIM UMR 7345, 13013 Marseille, France

Received: 12 October 2023 / Received in final form: 15 December 2023 / Accepted: 2 January 2024

**Abstract.** The Jules Horowitz Reactor (JHR) is an MTR under construction at the CEA Cadarache, France. Its design and future operation build upon the lessons learned from the OSIRIS MTR. The CEA intends to transfer the knowledge accumulated with the ISABELLE1 loop of OSIRIS to the ADELIN loop of the JHR, both dedicated to power-ramp-type irradiation experiments, the purpose of which is to test the resistance of PWR fuel rod cladding under extreme levels of stress. In this article, we revisit the ETALISA experiment, a heat balance measurement experiment performed in 1992 for calibrating power ramps in ISABELLE1. We use high-fidelity modelling and simulation tools, especially the neutron-gamma TRIPOLI-4<sup>®</sup> Monte Carlo transport code, to calculate the detailed components of the heat balance, correction terms, and uncertainties. Comparisons between the simulations and the experiments show a very good agreement in the total linear heat generation rate of 400 W/cm at high power. The computed  $2\sigma$  uncertainty is found to be 5%, a value essentially identical to the estimate derived in 1993 from an engineering approach. The use of modern simulation tools does not make it possible to improve upon this value, but provides a better understanding of the various components and corrections introduced in the total heat balance. The main limitations come from the ISABELLE1 online instrumentation, thermocouples and self-power neutron detectors, which set a limit on our very knowledge of the actual power ramp experimental conditions.

## 1 Introduction

Material Testing Reactors (MTR) are experimental irradiation reactors built to qualify structural materials and fuel rods, to improve the safety and performance of commercial power plants. MTR experiments are conducted under well-monitored and controlled conditions, with very high neutron flux in order to accelerate the irradiation damages in atomic structures. MTRs are designed to carry out irradiation experiments that meet well-defined steady-state or transient requirements, in order to obtain the validation-qualification data required to support the nuclear power industry [1].

MTR generally have a compact core with plate-type fuel elements cooled by water in forced convection, resulting in a high density of fission power in the core, therefore a high neutron flux density, inducing a high rate of damages in the materials under test. Irradiation experiments are conducted in special devices placed either in the core or in the surrounding reflector. A MTR reflector generally consists of water and beryllium or graphite,

which are excellent neutron moderators, efficiently slowing down neutrons. There is therefore a higher thermal neutron flux density in the reflector than in the core. The reflector serves to conduct mainly fuel irradiation experiments. Non-fuel material experiments, on the other hand, are generally done in the core.

From 1966 to 2015, the CEA operated the OSIRIS reactor in Saclay, one of the most reliable MTR in the world. Ramp tests were conducted in the ISABELLE Device [2], situated in the water reflector of OSIRIS. In 2015, OSIRIS was permanently shut down. As most MTRs in Europe are approaching retirement age or have already been shut down, it is becoming difficult to obtain the required experimental data [1]. The CEA is constructing the JHR (Jules Horowitz Reactor) at the CEA Cadarache [3], with the goal that it will become the most important European technological irradiation reactor of this century [4]. The design of the JHR largely builds upon the lessons learned from the operation of OSIRIS and its irradiation devices.

In particular, the CEA intends to transfer as much of the knowledge accumulated with the ISABELLE1 loop of OSIRIS to the ADELIN loop of the JHR. ISABELLE1

\* e-mail: [david.blanchet@cea.fr](mailto:david.blanchet@cea.fr)

and ADELINe are both fuel irradiation devices. They are designed to carry out fuel power ramping tests, a special type of irradiation experiments to test the resistance of PWR fuel rod cladding under extreme levels of stress induced by power transients. The goal is to improve our knowledge of PWR fuel element technological limits, especially those associated to Pellet-Cladding Interaction (PCI), a complex phenomenon [5]. These devices are placed in the reflector located at the periphery of the core, on mobile systems which can be positioned at a variable radial distance from the core, in order to modify the irradiation conditions, i.e., the Linear Heat Generation Rate (LHGR) in the experimental fuel samples. These devices are also equipped with instrumentation, making it possible to have a precise control of the irradiation conditions during power ramps.

The performances ultimately achieved with the ISABELLE1 loop, particularly with regard to the control of the irradiation conditions and the LHGR in the experimental rod, benefitted from the integration of many years of OSIRIS operation. The device was continuously improved since its commissioning in 1989 [6]. This optimisation was carried out by improving the instrumentation and experimental techniques. Given the limitations of modelling and simulation tools available at the time, simplified engineering-type approaches had to be used, and they had to be supplemented by the integration of multiple experimental data in order to achieve the target precision.

Today, a new generation of simulation and computing tools having high-fidelity modelling capabilities are available at the CEA and can be used to optimize the JHR irradiation conditions and the experiments hosted in the reactor. In particular, the irradiation conditions in the sample holding experimental devices positioned on Displacement Systems can be calculated with limited modelling simplifications and approximations.

The various sensors and measurement devices can also be modelled in situ. This instrumentation serves to guarantee the online control of the neutronic and thermohydraulic conditions during the power ramps and the power plateaus. The online irradiation measurements contribute to the control of the LHGR level and its variations with time. They are supplemented by pre- and post-irradiation measurements. Pre-irradiation measurements are used to calibrate the gamma heating and the neutron flux. Post-irradiation measurements serve to reconstruct the irradiation conditions.

The CEA sets out to achieve a high level of performance with the ADELINe loop immediately at the start of the JHR operation, which is foreseen at the beginning of the next decade. This high level of performance is the level reached with the ISABELLE1 device in the final years of the OSIRIS operation. This is a challenging goal, as there is limited validation data to assess the performance of the new calculation tools when used to model ADELINe in the JHR.

In this article, we revisit the power ramps carried out with the ISABELLE loop in OSIRIS some 30 years ago [7]. We do so using the new generation of CEA modelling and simulation tools. Such power ramps provide

valuable data for the validation of these tools. Our ultimate objective is to optimise the JHR experimental protocols, techniques and methods, in order to guarantee that the irradiation conditions, the LHGR and its variations are all within target requirements and operational margins.

Power ramp-type tests in MTR are described in Section 2. The OSIRIS reactor and the ISABELLE 1 device are presented in Section 3. Section 4 describes the control and monitoring of the ISABELLE irradiation conditions during the ETALISA power ramp. In Section 5, we describe the advanced methods used to model of the irradiation conditions in the ISABELLE device during the power ramp. Finally, in Section 6, we critically analyse our results.

## 2 Power ramp tests

In a PWR, the fuel cladding is an essential barrier against fission product release in the coolant, its integrity must therefore be assured. Without due precautions, several physical phenomena can occur, which can have adverse consequences:

- weakening of the cladding by corrosion;
- rupture of the cladding due to PCI;
- transition to a boiling crisis and dispersion of fragments of fuel pellets in the primary circuit;
- melting of fuel pellets.

PCI is the result of the combination of mechanical and chemical interactions between the UO<sub>2</sub> fuel pellets and the Zircaloy cladding. It is one of the general mechanisms of cladding rupture under normal operating conditions, especially during power changes, during restart or reactor manoeuvres [8]. Cladding failure is the primary cause of fuel rod damage and failure. PCI can lead to cladding rupture under the influence of molecules such as I, Cs and Cd in a material susceptible to Stress Corrosion Cracking (SCC), such as Zircaloy [9], subjected to an oxygen potential and an applied stress. SCC is the growth of cracks under the combined influence of non-cyclic tensile stress and a reactive environment. This phenomenon was discovered during testing of high-power Zircaloy-UO<sub>2</sub> fuel rods in the G.E. Test Reactor at Vallecitos in 1963 [10]. To control this phenomenon, fuel rod operating limits have been studied and implemented, as well as design modifications. The limits mainly concern the maximum ramp speed and maximum power increase that the fuel rods can withstand. The design modifications consist of changes applied to the inner surface of the cladding, pellet treatments and fuel fabrication [11].

Due to the complexity of the phenomena involved, predicting PCI reliably using simulations alone is a challenge. In practice, it is necessary to conduct experimental tests under various representative conditions in order to establish the rules and limits (margins) of admissible operation for each type of nuclear fuel [12]. Fuel power ramp tests are experiments carried out in MTRs to establish and validate these rules, explore operating limits, develop and test design modifications.

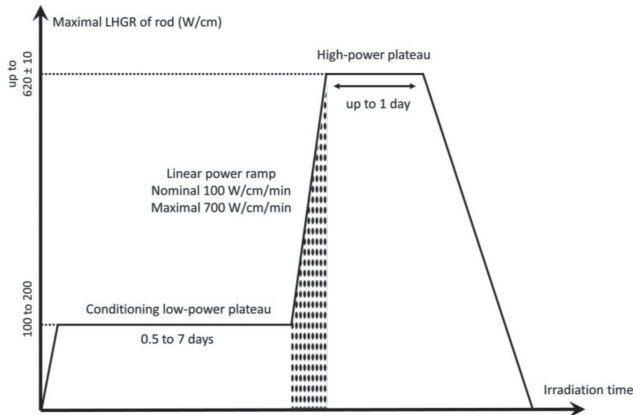


Fig. 1. Standard power ramp test time history [13].

Figure 1 shows a typical PWR power ramp test. It generally contains three irradiation phases: a low-power plateau, a linear power increase (ramp), and a high-power plateau.

During the low-power plateau, the experimental fuel rod is irradiated at a LHGR between  $100 \text{ W cm}^{-1}$  and  $200 \text{ W cm}^{-1}$ , depending on the need, for 0.5 to 7 days. The cladding outer surface temperature is maintained at  $330 \pm 10^\circ\text{C}$ . This initial phase is used to reproduce the PWR irradiation conditions.

The linear power ramp is generally obtained by moving the sample holder device by means of a displacement system placed in the reflector. The LHGR is increased by moving the experimental device horizontally towards the core vessel at a variable speed, in order to obtain a constant heating rate in the range between  $100 \text{ W cm}^{-1} \text{ min}^{-1}$  (nominal) and  $700 \text{ W cm}^{-1} \text{ min}^{-1}$  (maximum). The cladding surface temperature becomes stable at the saturated condition once the maximum linear power reaches  $350 \text{ W cm}^{-1}$ . This phase serves to explore the technological limit relating to fuel PCI in an incidental situation characterized by a rapid linear power increase.

During the final high-power plateau, the fuel rod is irradiated to reach an LHGR of up to  $620 \pm 10 \text{ W cm}^{-1}$ , for up to 1 day [13,14]. This final phase serves to explore the technological limit relating to fuel PCI in an incidental situation in which the linear power is up to six times higher than in normal PWR operation.

### 3 Ramp tests in the OSIRIS reactor

ISABELLE is a fuel irradiation device located in the eastern reflector of OSIRIS. This section briefly describes the OSIRIS core and the ISABELLE device.

#### 3.1 OSIRIS core

OSIRIS [2] was a light-water pool-type and open-core MTR operating at a nominal power of 70 MW. The compact core design ( $60 \text{ cm} \times 70 \text{ cm} \times 70 \text{ cm}$ ) consists of a square arrangement of plate-type fuel elements using uranium silicate ( $\text{U}_3\text{Si}_2\text{-Al}$ ) enriched to 19.75% in  $^{235}\text{U}$ .

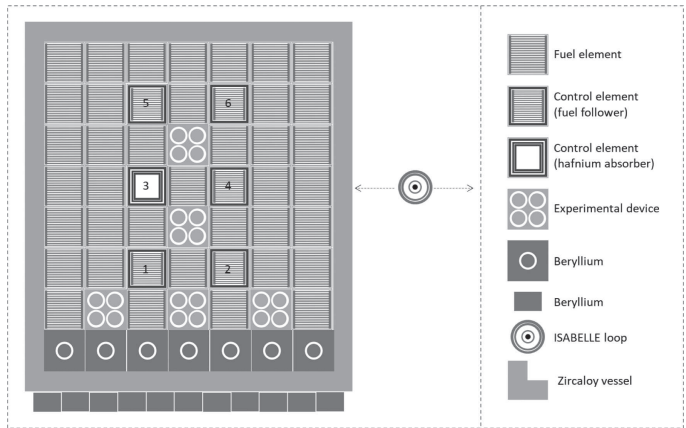


Fig. 2. OSIRIS core and ISABELLE loop in the eastern water reflector.

As shown in Figure 2, the core vessel contains 56 square elements of size 8.74 cm. The core is made of 38 standard fuel subassemblies, 6 control elements, up to 7 beryllium elements (located in the south side), and 5 in-core experimental positions charged of MOLFI Device producing medical radioisotopes or Material Device.

Each fuel element contains 22 fuel plates ( $5.57 \text{ cm} \times 0.051 \text{ cm} \times 63 \text{ cm}$ ). The fuel plates are equally spaced using borated aluminium stiffeners.

The control elements contain two sections: a hafnium section and a fuel follower. The hafnium neutron absorber is located in the top part. The fuel section of 17 fuel plates is similar to the standard fuel element assembly and is located in the bottom part. During a rod drop, the hafnium section is inserted into the reactor, capturing neutrons, while the fuel section is simultaneously withdrawn below the active part of the core, further reducing the fission rate and therefore the generation of neutrons. Thus, this design provides a dual neutronic effect.

On the south side of the core, the beryllium elements serve as a neutron reflector near the Material Device elements [15].

Unlike commercial PWRs, the operational temperature of water in an MTR is around  $30^\circ\text{C}$ .

OSIRIS operated up to 200 days per year, with a typical cycle length ranging from 3 to 5 weeks. During the refuelling outages, in-core experiment loading and unloading operations were carried out, as well as minor maintenance operations [2].

#### 3.2 ISABELLE loop

ISABELLE [6] is a moveable closed-loop water circuit independent of the reactor cooling circuit, located in the water reflector on the east side of the vessel (see Fig. 2). A typical experimental load is a short segment of a fuel rod, either fresh or irradiated in a PWR power plant and “remanufactured” in a hot laboratory. ISABELLE is designed to irradiate fuels under thermohydraulic and chemical conditions representative of those of a PWR.

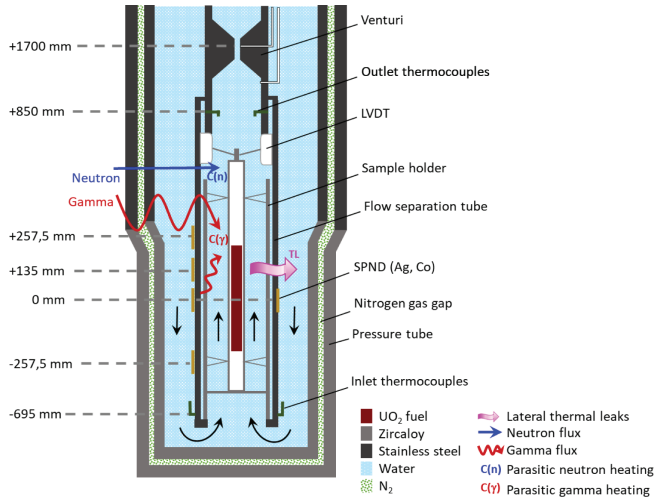


**Fig. 3.** Axial cross-section of the ISABELLE device equipped with measurement instrumentation.

In operating conditions, the ISABELLE coolant consists of demineralized water, degassed by heating, at a maximum pressure of 170 bar, a maximum inlet temperature of 315°C and a nominal flow rate of 0.2 kg/s.

A cut-away view of the ISABELLE device is shown in Figure 3. The mid plane of the fuel rod corresponds to the OSIRIS core midplane.

The pressure tube consists of two concentric cylindrical tubes, made of stainless steel in the upper part, extended in the lower part, in the zone under neutron flux, by two zircaloy tubes, separated by a nitrogen gas gap ensuring thermal insulation as well as a safety function as a pressure envelope.

The sample holder is the inner structure in which the experimental fuel rod is placed. A thin lamina of water provides thermal insulation between the sample holder and the flow separation tube, to minimize the radial heat losses between the hot and the cold legs of the cooling circuit. The internal arrangement ensures the separation of the inward and outward water flow. The water flows downwards in the external channel, between the pressure tube and the sample holder, then upwards in the internal channel to cool down the fuel rod.

The flow rate is measured using a venturi positioned at +1700 mm above the core mid plane.

Temperature measurements are achieved using two sets of thermocouples located at elevations of -700 mm and +850 mm relative to the core mid plane.

The thermal neutron flux is controlled and monitored using SPND (Self Powered Neutron Detector) with silver and cobalt emitters, located on the external surface of the flow separation tube, at the same elevation as the fuel rod. Four silver SPNDs and two cobalt SPNDs are located at the core mid-plane of OSIRIS to infer the power released by the fuel rod at the maximum flux plane. Two more silver SPNDs are placed at different elevations to obtain a measure of the axial distribution of the neutron flux. Three additional silver SPNDs are located at +135 mm

above the axial midplane to overcome any failure of the others.

The thermal expansion of the fuel rod is measured by means of an LVDT (Linear Variable Differential Transformer) elongation sensor [6].

## 4 Control and monitoring of the irradiation conditions

A diverse set of measurements is used to control the neutronic, hydraulic and thermal conditions of the experiment, before, during, and after the ramp.

Before the ramp tests, pre-irradiation measurements are carried out to predict the irradiation condition of the displacement system before loading the test device. These measurements make use of (i) a differential calorimeter [16] to infer the gamma heating, and (ii) a dosimetry system such as the system developed in ISIS, a zero-power mock-up of the OSIRIS reactor [17], to infer the neutron flux levels along the trajectory of the displacement system.

During the power ramps the power level plateaus, inlet temperature, outlet temperature, and mass flowrate [7] are measured online, from which the LHGR in the test section is inferred; the thermal neutron flux is also measured using SPND [7,18].

After the ramp, post-irradiation measurements are carried out, consisting of gamma spectrometry [6,19] and destructive radiochemical analyses [20]. From these analyses, the isotopic inventory of the irradiated fuel rod is found and used to reconstruct the reaction rates integrated during the experiments.

### 4.1 Neutron flux monitoring using SPND

During the linear power ramp, the LHGR is monitored using online measurements of the neutron balance by SPND with silver and cobalt emitters placed on the external flow separation tube. Delayed SPNDs like silver SPND are very sensitive to the thermal neutron flux [21], but their response time is too long for controlling transients. Prompt SPNDs like cobalt SPND, on the other hand, deliver an instantaneous response, but are too sensitive to gamma rays. A non-negligible signal drift was also observed with cobalt SPND during irradiations at constant power level, presumably due to gamma emission from activation products. However, the dynamic response of cobalt is virtually instantaneous and this is the reason why these detectors are used for ramp speed control, when linear power variations are significant ( $\sim 100 \text{ W cm}^{-1} \text{ min}^{-1}$ ). Silver SPNDs, on the other hand, are only sensitive to thermal neutrons; they can provide a very precise and stable response during irradiation at constant power, but with a fairly long response time. An anticipation method was therefore developed for silver SPNDs [22]. During a transient, this method yields a SPND response with only a short delay (see Fig. 4).

This anticipation method makes it possible to reduce the response time of the silver SPND from 10 min to a few seconds. The online control and monitoring of LHGR

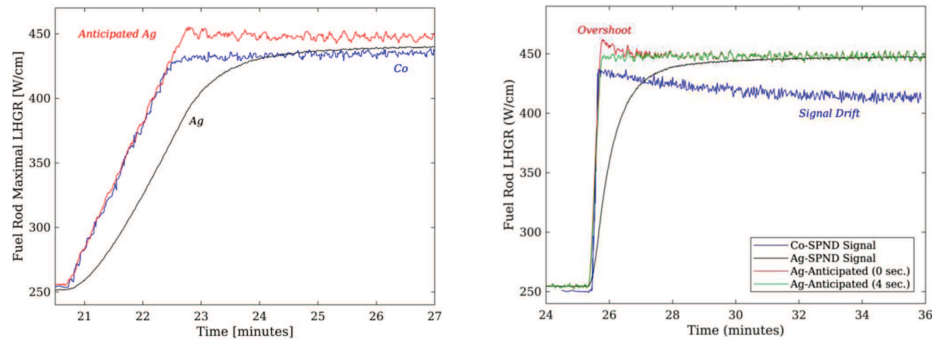


**Fig. 4.** Silver and Cobalt SPND signal during a nominal power ramp (left) and during a fast power ramp (right).

during the linear power ramp can therefore be done with silver SPND coupled with cobalt SPND. Before the ramp, during the low-power plateau, the cobalt SPNDs are calibrated with respect to the silver SPNDs, which in turn are calibrated with respect to the heat balance.

#### 4.2 Online power determination based on heat balance

The following heat balance equation gives the total power released by the fuel rod in the surrounding cooling water for the case of the irradiation plateau:

$$P(W) = QC_p(T_{\text{outlet}} - T_{\text{inlet}}) + TL - C(\gamma) - C(n) \quad (1)$$

In equation 1,  $Q$  ( $\text{kg}\cdot\text{s}^{-1}$ ) is the water flowrate in the cooling channel,  $T_{\text{inlet}}$  and  $T_{\text{outlet}}$  are the inlet and outlet temperatures of the water in the central channel, respectively, and  $C_p$  ( $\text{J}\cdot\text{kg}^{-1}\cdot\text{K}^{-1}$ ) denotes the specific heat capacity of water.  $TL$ ,  $C(\gamma)$  and  $C(n)$  are three correction terms which are illustrated in Figure 3 and explained below.

$TL$  is a correction term to account for lateral thermal leaks. A ferrule separates the inner water channel from the outer water channel. The sample holder and the flow separation tube are designed to create a thermal barrier against radial heat transfer between the inner and outer water channels. However, a small heat transfer still exists and must be accounted for in the heat balance equation.

$C(\gamma)$  is a correction term representing the parasitic gamma heating of water and structures in contact with water in the test channel. This heating is caused by the external source of gamma rays coming from the core and by the local source of gamma created by neutron interactions with the inner structures of the test channel. This gamma heating contribute to the coolant temperature rise in the test channel. However, as it does not correspond to the power released by the test fuel rod, this contribution must be subtracted off.

$C(n)$  is a correction term representing parasitic neutron heating of water and structures in contact with water in the test channel. This parasitic heating is caused by the neutron flux coming from the core and from the test fuel rod. This neutron heating is not directly related to the power released by the test fuel rod. Therefore, as it contributes to water heating in the central channel, it must be subtracted off.

In the following, we discuss the various means of estimating the heat balance correction terms and the corresponding uncertainties.

#### 4.3 Calibrations using experimental data

In the years of the OSIRIS operation, as the simulation tools and computing resources were much more limited than today, gamma heating had to be experimentally calibrated by engineering methods based on FADIL factors and pre-irradiation calorimetric measurements. A graphite-based double differential calorimeter was designed so that it can replace the ISABELLE loop on the displacement system, in order to measure gamma heating as a function of the distance from the core. Gamma heating was inferred from the temperature difference measured between pairs of cells inside the calorimeter, one cell being surrounded with graphite, the other cell with nitrogen gas. Details about the measurement technique can be found in [16,23,24]. Then, an engineering method based on FADIL factors (a former library of nuclear heating equivalence factors in various materials [25]) was used to translate the gamma heating in graphite measured by the calorimeter into the gamma heating of the ISABELLE structural materials. The FADIL factors are plotted in Figure 5. The uncertainty associated to this FADIL transfer factor method was estimated to be at least 15% at  $2\sigma$ .

The thermal leakage  $TL$  can be calculated with the REFLET thermal code [6]. The CEA estimates the corresponding uncertainty to be no more than 10% at  $1\sigma$ , as a result of the heat exchange models used to calculate  $TL$ . In the case of ISABELLE,  $TL$  represents up to 4% of the total heat balance. The various models used in the REFLET code, including the heat transfer correlations, were tested and validated against experimental data. Thermal leakages and radial heat losses were assessed by the REFLET code and validated with the help of multiple dedicated experiments. A set of calibration experiments considered the irradiation of a dummy metal rod for instance. The heat exchange models were verified by using an out-of-pile loop with an electrically heated rod [7].

ETALISA (*ÉTA*lissage ISABELLE) [6] is the name of an ISABELLE power ramp calibration experiment that was performed in 1992 in order to qualify the online

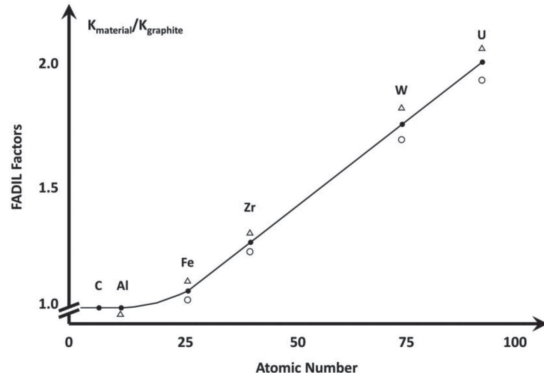


**Fig. 5.** FADIL library of nuclear heating equivalence factors in various materials.

**Table 1.** Inter-laboratory comparison of LHGR measurements for ETALISA high level plateau [7].

Method	LHGR $\pm 2\sigma$ (W/cm)
ISIS dosimetry	410 $\pm$ 22
OSIRIS $\gamma$ spectrometry	410 $\pm$ 42
LAMA $\gamma$ spectrometry	406 $\pm$ 44
Isotopic analysis (U/Nd)	405 $\pm$ 12
Heat balance	409 $\pm$ 22

power measurements by heat balance. A fresh fuel rod, with a well-known isotopic composition, was irradiated at a constant high power of about 400 W/cm during 13 days. The heat balance measurements were compared with the results obtained by three independent fission power measurement methods involving different laboratories: dosimetry, gamma spectrometry and destructive radiochemical analyses. From these post-irradiation analyses, the isotopic inventory of the irradiated fuel rod was used to reconstruct the reaction rates integrated during the experiments. These measurements were corrected to account for the gamma heating previously measured by calorimetry (gamma heating represents 2 to 3% of the total). Table 1 compares the results obtained by the different methods with the associated  $2\sigma$  uncertainties. The good agreement of the results thus obtained enabled one to qualify the average-power measurement method by heat balance.

The axial power distribution was measured during post-irradiation examinations by gamma-ray spectrometry of short-lived fission products (e.g. Zr, Nb, La, Ba). The maximum linear power was then deduced by dividing the heat balance measurement by the fissile column length and by the axial power form factor.

## 5 Improved modelling of the irradiation conditions

In this section, we successively describe the models we utilized to describe and calculate: (i) the irradiation condi-

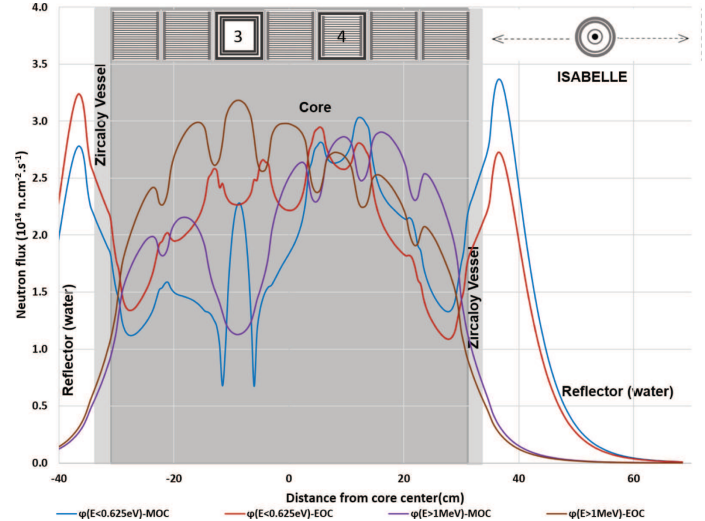


**Fig. 6.** Variations of the fast neutron flux ( $E > 1$  MeV) and the thermal neutron flux ( $E < 0.625$  eV) distributions in the OSIRIS core, from the Middle-of-Cycle to the End-Of-Cycle during the ETALISA experiment.

tions in the OSIRIS core; (ii) the detailed nuclear heating calculations in the ISABELLE loop internals; (iii) uncertainties.

In this work, extensive use was made of the TRIPOLI-4<sup>®</sup> continuous-energy Monte Carlo transport code Version 4.11 associated with the JEFF3.1.1 nuclear library (Version CEAV512) [26].

### 5.1 Full core neutronics analysis

A very detailed, high-fidelity TRIPOLI-4<sup>®</sup> model of the OSIRIS core was set up, corresponding to the middle of the cycle (MOC), the core being critical with the control element #3 fully inserted.

Figure 6 shows the computed fast and thermal neutron fluxes along a radial traverse in the water reflector, in an undisturbed situation, i.e., without the ISABELLE loop. The eastward flux tilt is clearly visible, leading to a higher thermal flux peak in the eastern reflector and a corresponding lower peak in the western reflector. The thermal and fast fluxes show variations in the core at the interfaces between subassemblies, as expected. We observe that the fast flux attenuates exponentially in the reflector. The thermal flux follows the same trend, but only after reaching a maximum value. Indeed, the moderation of the fast neutrons generated in the core produces a significant increase in the thermal neutron flux in the reflector, with a peak close to the vessel outer surface (approximately 2 cm away).

In the standard configuration, the thermal flux peak decreases in the eastern reflector but increases in the western reflector. A slightly asymmetrical radial flux profile is observed due to the heterogeneous fuel burn-up rate distribution (ranging from 10 to 80 GWd/t in this row). For the particular traverse shown in Figure 6, the fuel assemblies having relatively lower burnups generate relatively

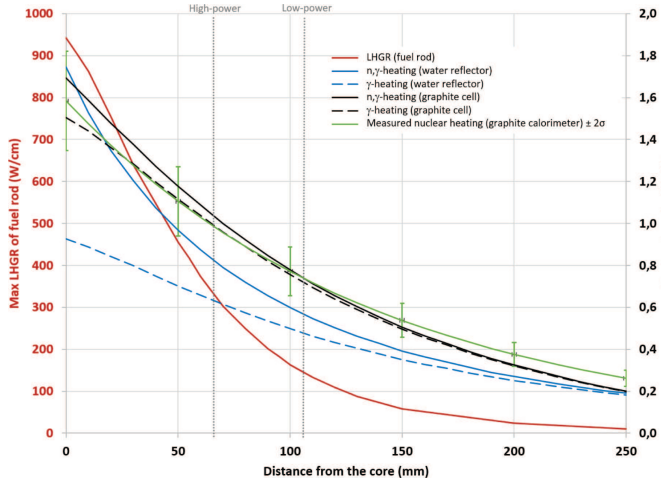


**Fig. 7.** Maximal LHGR of the ISABELLE fuel rod and nuclear heating in the OSIRIS water reflector and in the calorimetric graphite cell calculated by TRIPOLI-4<sup>®</sup>, compared to the measured gamma heating in graphite (green curve).

stronger neutron fluxes. We conclude that operating the OSIRIS core in tilted mode (by inserting control element #3) leads to a  $\sim 20\%$  radial redistribution of the neutron flux from the western reflector to the eastern reflector, where the displacement system of the ISABELLE device is located, favoring the irradiation of the hosted experiments. This mode of operation was the one used most of the time to create the power ramps in OSIRIS.

## 5.2 Detailed nuclear heating calculations

The TRIPOLI-4<sup>®</sup> code was also used to model the irradiation conditions of the ISABELLE loop.

The distance between the ISABELLE pressure tube and the zircaloy core vessel is denoted as  $d$ .

Nuclear heating in ISABELLE is calculated for different recoil positions of the displacement system, from the fully advanced position ( $d = 0$ ) to the fully retracted position ( $d = 250$  mm). The maximal LHGR of the test fuel rod is plotted as a function of the distance to the vessel in Figure 7. The gamma heating attenuation in the water reflector is represented on the same figure. The LHGR attenuates nearly a hundredfold across the displacement system range, while the gamma heating attenuates by only a factor five, as gamma flux attenuates more slowly than neutron flux in the water reflector.

Figure 8 shows a synoptic diagram of the calculation route we used for computing all the components of the heat deposited in the central channel of ISABELLE. It is based on (i) the APOLLO2 lattice physics code, (ii) the CRONOS2 full code calculation code, (iii) the DARWIN code for delayed gamma source calculations, (iv) the JEFF3.1.1 nuclear data library, and (v) the TRIPOLI-4<sup>®</sup> Monte Carlo code. The TRIPOLI-4<sup>®</sup> code is actually used in different calculation modes: critical ( $n, \gamma$ ) coupled transport simulation to calculate the neutron heating and the prompt gamma heating in the device; source-mode

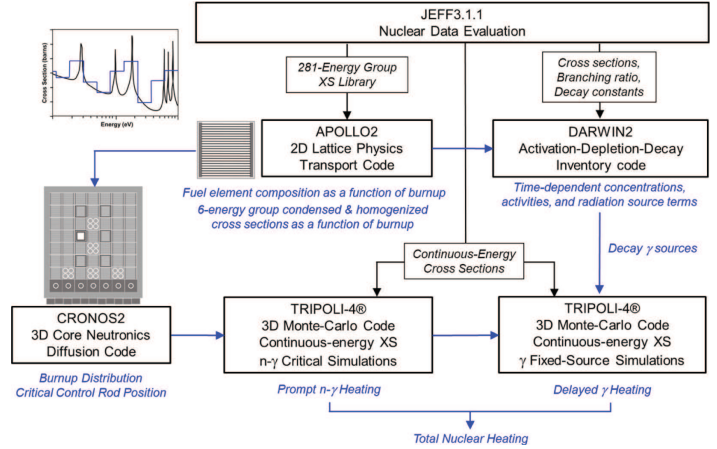


**Fig. 8.** Reference flow diagram used at the CEA for nuclear heating calculations.

( $\gamma$ ) transport simulation to calculate the delayed gamma heating in the device, the input delayed gamma sources being obtained from DARWIN. These data and codes are extensively used at the CEA for various applications, they benefit from an extensive validation [27–30].

During the ETALISA experiment, the ISABELLE rod was irradiated for 13 days in the high-power plateau to calibrate the heat balance measurement. We modelled this experiment with the code system of Figure 8. ISABELLE was located at  $d = 9.8$  cm (resp.  $d = 5.7$  cm), in the low (resp. high)-power plateau, as indicated in Figure 7.

Table 2 compares the nuclear heating calculated by TRIPOLI-4<sup>®</sup> – DARWIN in the graphite cell of the calorimeter before the ETALISA experiment. The neutron heating has a non-negligible contribution (11% at  $d = 0$ ) to the total heating when the displacement system is close to the core vessel. However, as all the nuclear heating measured by calorimeter is considered to be gamma heating in the engineering method, the calorimeter is expected to overestimate gamma heating in the advanced positions.

Table 3 shows the nuclear heating components calculated with the data and code system illustrated in Figure 8. The results of the engineering method, which was originally used in 1992, are also shown for comparison purposes. Based on experimental data from the graphite calorimeter (represented by the green line in Fig. 7), the engineering method helps to translate the measured nuclear heating to the ISABELLE water channel and structure heating using the FADIL factor technique. The details of nuclear heating calculated in the water channel, zircaloy and steel structures of ISABELLE device are shown. The parasite gamma heating,  $C(\gamma)$ , refers to prompt gamma heating and delayed gamma heating by decay of fission products in the OSIRIS core and in the local (ISABELLE) fuel rod, as the delayed gamma heating by decay of activation products is negligible. The parasite neutron heating,  $C(n)$ , refers to neutron heating.  $C(\gamma)$  and  $C(n)$  in the central water channel are used to correct the heat balance.

The engineering method provides a good estimate of gamma heating in the water channel, therefore the cor-



**Table 2.** Components of nuclear heating calculated by TRIPOLI-4<sup>®</sup> in the graphite cells of the calorimeter.

Heating components	Graphite calorimeter			
	Advanced position $d = 0$		Recoiled position $d = 250$ mm	
	Heating (W/g)	Contribution (%)	Heating (W/g)	Contribution (%)
Neutron	0.19	11%	0.002	1%
Prompt $\gamma$	1.23	73%	0.19	93%
Delayed $\gamma$ (fission products)	0.23	14%	0.01	5%
Delayed $\gamma$ (activation products)	0.04	2%	0.002	1%
Total	1.69	100%	0.20	100%

**Table 3.** Components of nuclear heating in the ISABELLE structure and summary of the heat balance in the ETALISA experiment, revisited with the high-fidelity modelling using TRIPOLI-4 and compared with the original engineering method.

Plateau	Method	Nuclear Heating of ISABELLE (W/g)				Heat Balance (W)					Max LHGR W/cm
		Neutron	Gamma			Corrections		REFLET			
			Water	Water	Steel	Zircaloy	$C(\gamma)$	$C(n)$	TL	Q.Cp. $\Delta T$	
Low	High-Fidelity	0.36	0.71	0.67	0.77	-90.9	-32	-67.5	5844.7	5654.3	176
	Engineering	-	0.78	0.84	0.99	-90.8	-113.7	-68.5	5845.5	5572.5	173
	Discrepancy (%)	-	10%	25%	29%	0%	255%	1.5%	0.0%	-1.4%	-1.4%
High	High-Fidelity	0.81	1.08	1.02	1.19	-125.3	-85.2	107.7	13172.6	13069.8	409
	Engineering	-	1.05	1.12	1.33	-118.6	-263.1	117.9	13155.6	12891.8	403
	Discrepancy (%)	-	-3%	10%	12%	-5%	209%	9.5%	-0.1%	-1.4%	-1.4%

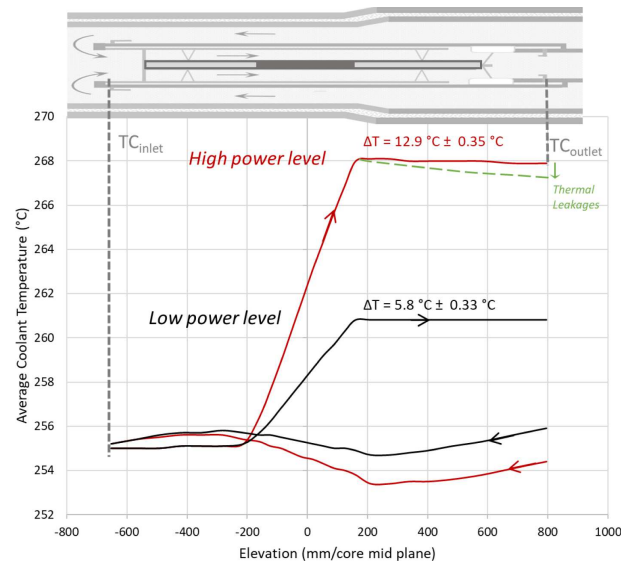
rective term  $C(\gamma)$  is almost identical to the one obtained with reference TRIPOLI-4<sup>®</sup> simulations. Although the engineering method overestimates structural heating, leading to temperatures which are too high, this has a rather limited impact on the corrective terms related to thermal leakage. The most notable differences concern the correction for parasitic neutron heating  $C(n)$ . However, the consequences are minor as this term represents less than 2% of the total heat balance.

The high-fidelity modelling approach provides accurate nuclear heating estimates and a better understanding of the various correction terms in the heat balance equation. However, in the end, the observed discrepancy with the engineering method amounts to only -1.4% in the total heat balance.

The maximal LHGR calculated by TRIPOLI-4<sup>®</sup> is  $400 \pm 4.5$  W/cm at  $2\sigma$ . This state is considered a very stable level but subject to fluctuations, a situation similar to the ETALISA experiment.

Taking the form factor  $ff \approx 1.09$  (maximal LHGR/average LHGR) and the axial length of the fuel rod  $L = 35$  cm into account, the maximum LHGR derived from this heat balance is therefore  $176$  W.cm<sup>-1</sup> in the low-power plateau and  $409$  W.cm<sup>-1</sup> in the high-power plateau.

Figure 9 shows the axial water temperature in the inner and outer channels calculated by REFLET. The outlet-inlet temperature difference is  $5.8^\circ\text{C}$  in the low-power plateau and  $12.9^\circ\text{C}$  in the high-power plateau. The uncertainties quoted in Figure 9 regarding the temperature differences will be discussed in the next section.

**Fig. 9.** Flowing water channel temperature during ISABELLE power level plateaus, modelled with REFLET simulations.

The thin water layer between the sample holder and the flow separation tube is an important design feature. This water gap acts as a thermal insulation barrier to limit the heat exchange between the hot and cold legs of the water circuit. Without this water layer, the thermal leaks would increase, as illustrated in Figure 9, and this would result in a temperature difference that would not

**Table 4.** Uncertainties at  $2\sigma$  in the power measured by heat balance.

Parameters		Uncertainties ( $2\sigma$ %)			
		High-power plateau		Low-power plateau	
		Engineering	High-Fidelity	Engineering	High-Fidelity
Flow Rate Measurement	$Q$	0.6%	0.6%	0.6%	0.6%
Calorific Capacity	$Cp$	0.2%	0.2%	0.2%	0.2%
Temperature difference	$\Delta T$	5.4%	5.4%	12.0%	12.0%
Thermal Leakage	$TL$	0.8%	0.8%	0.8%	0.8%
Gamma Correction	$C(\gamma)$	0.8%	0%	0.8%	0%
Neutron Correction	$C(n)$	0.8%	0%	0.8%	0%
Avg LHGR	$P$	5.6%	5.5%	12.1%	12.1%

correspond to the actual heat released by the fuel rod. This confirms the importance of performing calibration tests to adjust the thermal leakage model to the actual experimental conditions.

### 5.3 Uncertainty assessment

In this section, we evaluate the modelling uncertainties to be assigned to the various terms in equation 1.

An important source of uncertainty in the heat balance comes from the ISABELLE inlet-outlet temperature difference. ISABELLE is equipped with 8 thermocouples at the inlet and 6 thermocouples at the outlet [6]. The measured inlet-outlet temperature difference  $\Delta T$  is inferred from two sets of data:

- the average of three direct temperature differences  $\Delta T$  (three pairs of opposite input-output thermocouples);
- the difference between the average of three outlet temperatures ( $TC_{\text{outlet}}$ ) and five inlet temperatures ( $TC_{\text{inlet}}$ ).

The standard uncertainty (systematic error) in the temperature measurement from a thermocouple  $u_{TC}$  is  $0.580^\circ\text{C}$ , according to CEA experts [31].

The uncertainty  $u_{\Delta T_{\text{measured}}}$  in  $\Delta T_{\text{measured}}$  is calculated from  $u_{TC_{\text{inlet}}} = u_{TC_{\text{outlet}}} = u_{TC} = 0.580^\circ\text{C}$ :

$$\begin{aligned}
 & u_{T_{\text{measured}}} \\
 &= \sqrt{\left(\frac{\sqrt{u_{TC_{\text{outlet}}}^2 + u_{TC_{\text{inlet}}}^2}}{\sqrt{3}}\right)^2 + \left(\frac{u_{TC_{\text{outlet}}}^2}{3} + \frac{u_{TC_{\text{inlet}}}^2}{5}\right)^2} \\
 &= 0.317^\circ\text{C} \quad (2)
 \end{aligned}$$

The uncertainty  $u_{\Delta T}$  in the temperature difference  $\Delta T$ , comes from:

- the uncertainty in the measured temperature difference  $u_{\Delta T_{\text{measured}}} = 0.317^\circ\text{C}$ ;
- the intrinsic uncertainty in the “very stable” irradiation level plateau [31], from the fluctuation measured during the experiment or from the uncertainty of the LHGR calculated by TRIPOLI-4<sup>®</sup>:  $u_{\text{fluctuation}} = 0.145^\circ\text{C}$ ;

- the uncertainty in the convergence precision of the REFLET calculation (0.1% in this study).

The resulting combined uncertainty is  $u_{\Delta T} = 0.349^\circ\text{C}$ , corresponding to a relative standard deviation of 6% (resp. 2.7%) in the low (resp. high)-power plateau.

Table 4 summarizes the uncertainties associated with the power measured by the heat balance technique.

CEA estimated the uncertainty in the water flowrate to be 0.3% at  $1\sigma$  and the uncertainty in the water specific heat capacity to be 0.1% at  $1\sigma$  [31,32].

The uncertainty in  $C(\gamma)$  is  $\sim 10\%$  at  $1\sigma$  due to the combined uncertainty in the gamma heating measurement (7.5% at  $1\sigma$ ) and in the FADIL factor technique (7.5% at  $1\sigma$ ). Since  $C(\gamma)$  represents up to 4% of the heat balance, the resulting uncertainty is 0.4%.

The  $1\sigma$  uncertainty in  $C(n)$  is estimated to be 20%. This correction term accounts for less than 2% of the heat balance, so the resulting uncertainty is 0.4%.

The quoted uncertainty associated with the high-fidelity models is small, as only the statistical convergence of Monte-Carlo simulations is considered. In particular, errors and uncertainties arising from nuclear data are not considered in this study. Indeed, for ascertaining the relative differences between the engineering method and the high-fidelity approach, nuclear data uncertainties can be ignored since they contribute equally to both. The neutron calculation tools presented in Figure 8 have also benefited from an extensive validation work, including the AMMON [30] mock-up experiments in the EOLE reactor. The calculation methods used to analyse these experiments are the same as those used in the present study. The maximum calculation-measurement deviations found in nuclear heating estimates did not exceed  $(C/E-1) \approx -8\% \pm 12\%$  ( $2\sigma$ ) [33]. The observed discrepancies were mostly attributed to nuclear data uncertainties combined with measurement uncertainties.

As explained in Section 4.2, the uncertainty in  $TL$  is the uncertainty coming from the REFLET heat exchange models, not exceeding 10%. Since  $TL$  represents up to 4% of the heat balance, the resulting uncertainty is 0.4%.

## 6 Discussion

The use of modern high-fidelity modelling and simulation tools for analyzing the ISABELLE loop heat balance measurement during ramp experiments has made it possible to find improved estimates of various correction terms and the corresponding uncertainties. The uncertainty associated with parasite gamma heating model is reduced from 10% to 2% at  $1\sigma$  and the uncertainty associated to energy deposited correction model is reduced from 20% to 3% at  $1\sigma$ .

The total heat balance modelling uncertainty is at the same level as that of the ISIS dosimetry results, much lower than OSIRIS/LAMA  $\gamma$  spectrometry but still higher than that of the isotopic analyses.

We observe that the total heat balance modelling uncertainty of 5.5% (Tab. 4) is essentially identical to the experimental heat balance measurement uncertainty shown in Section 4.2 (about 5.4% at  $2\sigma$ ). The temperature difference is the leading contribution in both cases. We conclude that the recommended course of action for reducing the total heat balance uncertainty is to decrease the uncertainty in the inlet-outlet temperature difference, for example by using more thermocouples.

The uncertainty in the temperature difference can be reduced to 3.90% by using 10 pairs of inlet-outlet thermocouples (three pairs measuring temperature differences and seven pairs measuring average inlet/outlet temperature). This will be the case for the ADELINe irradiation device in the JHR reactor.

It would be desirable to further reduce this uncertainty to 2.78% by using 20 pairs of thermocouples, at a level better than all the experimental measurements revisited. However, this means that 40 thermocouples would have to be placed in the central channel, arranged in a ring. Such a ring would have a minimal thickness of about 5 mm, which is likely to perturb the thermal neutron flux. Additionally, using such a large number of thermocouples may not be possible for reasons of space constraints.

The duality between precision and delay for the anticipated signal of silver SPND is the major limitation of such delayed SPNDs for online control of LHGR during the linear power ramp. The anticipation method makes it possible to reduce the response time of the silver SPND from 10 mins to 4 s, obtaining an anticipated signal proportional to the LHGR. However, 4 s is still non-negligible during a fast linear ramp which last only 20 s. The coupling with cobalt SPND or numeric modelling in Section 5.2 could help improve this situation for a better online control of the LHGR during linear power ramps.

## 7 Conclusion

We revisited the ETALISA power ramp calibration experiment conducted in 1992 in the ISABELLE loop in the OSIRIS reactor. We took advantage of the extended modelling capabilities available in our current modelling simulation tools, combined with high-performance computers, to set up high-fidelity models of the reactor and the exper-

iment. Using the Monte-Carlo code TRIPOLI-4<sup>®</sup> together with the JEFF3.1.1 nuclear data library, we were able to compute the irradiation conditions of the ISABELLE loop on the displacement system with a statistical uncertainty of less than 4% at  $2\sigma$ .

The heat balance in the test fuel rod was modelled and computed with REFLET and TRIPOLI-4<sup>®</sup>. We were able to calculate various correction terms impacting this heat balance, as well as the corresponding uncertainties. The calculations correctly predict the measured LHGR at high power, the discrepancy being only 1.4%. The total calculation uncertainty is 5.5% at  $2\sigma$ . Remarkably, this calculation uncertainty is essentially equal to the experimental uncertainty assessed in 1993 and revised in 2005, which largely relied on an engineering approach and on operational feedback. The outlet-inlet water temperature difference along the ISABELLE central channel is the dominant source of uncertainty. Therefore, the most efficient way of reducing the total uncertainty would be to improve our knowledge of this temperature difference, for instance by using more thermocouples. However, the number of thermocouples is ultimately limited by space constraints.

Another limitation comes from the necessary trade-off between precision and delay in the silver SPND measurements, which induces some uncertainty in our knowledge of the actual power ramp conditions, and therefore in the online control of the LHGR in the test fuel rod. One way of improving this control would be to develop a real-time coupled simulation model of the SPND.

These results strongly suggest that, in order to achieve a high level of performance with the ADELINe loop immediately at the start of the JHR operation, comparable with the level of performance reached with ISABELLE1 in the final years of the OSIRIS operation (heat balance known to within 5% at high power), implementing high-fidelity calculation models will not be sufficient. It will be essential to have access to reliable experimental information, in the form of a sufficient number of thermocouples and fast-responding SPNDs, in order to assure a high-quality online control of the LHGR in the test fuels rod and its variations during the successive phases of the power ramps.

In future work, we will use the results of this study to establish the conditions to be imposed upon the JHR and ADELINe instrumentation and simulation models in order to have sufficient control of the irradiation conditions in the displacement system, so that the LHGR in the irradiated rods can be inferred with a  $2\sigma$  uncertainty of 5% or better in the high-power plateau, knowing that we will not have the analogue of the ETALISA experiment for ADELINe.

## Funding

This research did not receive any specific funding.

## Conflicts of interest

The authors declare that they have no competing interests to report.

## Data availability statement

This article has no associated data generated and/or analyzed/Data associated with this article cannot be disclosed due to legal/ethical/other reason.

## Author contribution statement

Yifan Peng implemented the TRIPOLI-4® model and wrote the first version of the paper. David Blanchet reviewed and edited the paper. Robert Jacqmin reviewed the paper and supervised the work from the CEA side. Jérôme Julien managed the CEA project. Joël Rosato supervised the work from the Aix-Marseille University side. All authors discussed the results and contributed to the final manuscript.

## References

1. S. Loubière, G. Bignan, D. Iracane, Sustaining material testing capacity in France: from OSIRIS to JHR, IGORR, October 2009 (2009)
2. CEA, Les réacteurs nucléaires expérimentaux, monographie (online) [https://www.cea.fr/multimedia/Documents/publications/monographie-nucleaire/CEA\\_Monographie9\\_Reacteurs-nucleaires-experimentaux\\_2012\\_Fr.pdf](https://www.cea.fr/multimedia/Documents/publications/monographie-nucleaire/CEA_Monographie9_Reacteurs-nucleaires-experimentaux_2012_Fr.pdf)
3. G. Bignan, X. Bravo, P.M. Lemoine et al., The Jules Horowitz Reactor: a new high performances European MTR with modern experimental capacities: toward an international user facility, IGORR, October 2013 (2013)
4. P.C. Camprini, M. Sumini, C. Artioli, et al., Power Transient Analyses of experimental in-reflector devices during safety shutdown in Jules Horowitz Reactor (JHR), PHYSOR, April 2012 (2012)
5. S. Martin, G. Bignan, Sustaining material testing capacity in France: from OSIRIS to JHR, in *International Conference on Research Reactors: Safe Management and Effective Utilization*, November, (2011), pp. 14–18
6. D.J. Moulin, Contrôle des conditions neutroniques et thermohydrauliques des rampes de puissance dans une boucle d'irradiation de combustibles de réacteur à eau pressurisée, Ph.D. thesis, Institut National Polytechnique, Grenoble, 1993
7. A. Alberman, M. Roche, P. Couffin, et al., Technique for power ramp tests in the ISABELLE 1 loop of the OSIRIS reactor, Nucl. Eng. Design. **168**, 293 (1997)
8. EPRI, Effect of Startup Ramp Rate on Pellet-Cladding Interaction of PWR Fuel Rods, Tech. rep. TR-112140-V2, Apr 09 (1999)
9. R. Adamson, B. Cox, J. Davies et al., *Pellet-Cladding Interaction (PCI and PCMI). ZIRAT -11 Special Topic Report* (Advanced Nuclear Technology International, Sweden, 2006)
10. B. Cox, Pellet clad interaction (PCI) failures of Zirconium alloy fuel cladding – A review, J. Nucl. Mater. **172**, 249 (1990)
11. D. Rozzia, B. Boer, F. Belloni et al., *Predictability of Fuel Failure due to Pellet Cladding Interaction Based on PWR Over Ramp Experimental Programme* (NENE, 2018)
12. EPRI, PCI Analyses and Startup Ramp Rate Recommendations for Westinghouse Fuel in Exelon PWRs, Tech. rep. TR-1012915, Palo Alto, CA (2006)
13. C. Blandin, J. Estrade, C. Colin et al., *Fuel and material irradiation hosting systems in the Jules Horowitz Reactor* (IGORR, October, 2013)
14. S. Gaillot, G. Cheymol, J. Brinster et al., *Fuel Irradiation Devices Test of Sealed Passages with Optical Fibres in Support of the Development of Innovative Instrumentation* (IGORR, March, 2019)
15. A. Peron, Contribution à l'Amélioration des Méthodes d'Évaluation de l'Échauffement Nucléaire dans les Réacteurs Nucléaires à l'Aide du Code Monte-Carlo TRIPOLI-4®, Ph.D. thesis, Université Paris-Sud, Ecole doctorale Modélisation et Instrumentation en Physique, Energie, Géosciences et Environnement, Paris, 2014
16. D. Blanchet, M. Antony, H. Carcreff, et al., Assessment of irradiation performance in the Jules Horowitz Reactor (JHR) using the CARMEN measuring device, in *EPJ Web of Conferences* (EDP Sciences, 2021), pp. 04010
17. G. Bignan, J-Y. Blanc, P. Chaix, The CEA scientific and technical offer as a designated ICERR (International Center based on Research Reactor) by the IAEA: first feedback with the prime Affiliates, IGORR 2017 and IAEA workshop on safety reassessment of research reactors in light of the lessons learned from the Fukushima Daiichi accident (J7-TR-54790), December (2017)
18. L. Vermeeren, J. Dekeyser, P. Gouat, et al., Qualification of the on-line power determination of fuel elements in irradiation devices in the BR2 reactor, Scientific Rep.- SCK. CEN-BLG-1006 (2005)
19. P.A. Demkowicz J.D. Hunn, R.N. Morris et al., AGR-1 post irradiation examination final report, Tech. rep. No. INL/EXT-15-36407 (Idaho National Lab.(INL), Idaho Falls, ID (United States), 2015)
20. J.M. Harp, H.J.M. Chichester, and L. Capriotti, Postirradiation examination results of several metallic fuel alloys and forms from low burnup AFC irradiations, J. Nucl. Mater. **509**, 377 (2018)
21. L. Vermeeren, *Neutron and Gamma Sensitivities of Self-powered Detectors: Monte Carlo modelling* (ANIMMA, April, 2015)
22. D.J. Moulin, Dynamic compensation of the Silver self-powered neutron detector in the ramp program at the OSIRIS reactor, ASTM Spec. Tech. Publ. **1228**, 255 (1994)
23. D. Fourmentel, C. Reynard-Carette, A. Lyoussi, et al., Nuclear heating measurements in material testing reactor: A comparison between a differential calorimeter and a gamma thermometer, IEEE Trans. Nucl. Sci. **60**, 328 (2013)
24. H. Carcreff, L. Salmon, F. Malouch, Recent developments in nuclear heating measurement methods inside the OSIRIS reactor, Nucl. Instrum. Methods Phys. Res., Sect. A **942**, 162310 (2019)
25. K.F. Mecheri, Energie déposée par le rayonnement gamma dans un réacteur d'essai – Mesures calorimétriques et calculs, Ph.D. thesis, Institut National Polytechnique, Grenoble, 1977
26. E. Brun, F. Damian, C.M. Diop, et al., Tripoli-4®, CEA, EDF and AREVA reference Monte Carlo code, Ann. Nucl. Energy. **82**, 151 (2015)
27. A. Péron, F. Malouch, C. M. Diop, Improvement of nuclear heating evaluation inside the core of the OSIRIS material testing reactor, EPJ Web of Conf. EDP Sci. **106**, 05006 (2016)

28. C. Vaglio-Gaudard, O. Leray, M. Lemaire, et al., First feedback with the AMMON integral experiment for the JHR calculations, EPJ Web Conf. EDP Sci. **42**, 05001 (2013)
29. J. Di Salvo, C. Vaglio-Gaudard, A. Gruel, et al., The AMMON experiment in EOLE zero power facility: a challenging program devoted to the neutron and photon physics: Physor 2014, J. Nucl. Sci. Technol. **52**, 1034 (2015)
30. J.C. Klein, N. Thiollay, J. Di Salvo, et al., *AMMON: an experimental program in the EOLE critical facility for the validation of the Jules Horowitz Reactor neutron and photon HORUS3D calculation scheme* (IGORR, October, 2009)
31. N. Devictor, (Personal communication), 2005
32. S. Bendotti, (Personal communication), 1994
33. M. Lemaire, Validation des calculs d'échauffements photoniques en réacteur d'irradiation au moyen du programme expérimental AMMON et du dispositif CARMEN, Ph.D. thesis, Université Aix-Marseille, Ecole Doctorale Physique et Sciences de la Matière, Aix-Marseille, 2015

**Cite this article as:** Yifan Peng, David Blanchet, Robert Jacquemin, Jérôme Julien, Joël Rosato. High-fidelity models for the online control of power ramps in fuel displacement systems – Revisiting the ISABELLE experiment in the OSIRIS Material Testing Reactor, EPJ Nuclear Sci. Technol. **10**, 3 (2024)